Journal of Molecular Spectroscopy 409 (2025) 111998

Contents lists available at ScienceDirect

Journal of Molecular Spectroscopy

journal homepage: www.elsevier.com/locate/yjmsp

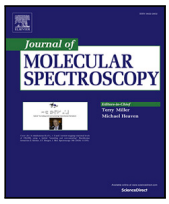

Empirical rovibrational energy levels for carbon disulfide

Tanvi Sattiraju, Jonathan Tennyson *

Department of Physics and Astronomy, University College London, Gower Street, London WC1E 6BT, UK

ARTICLE INFO

Keywords:
Energy levels
Carbon disulfide
MARVEL
Spectroscopic network

ABSTRACT

An analysis of the measured rovibrational transitions is carried out for the $^{12}C^{32}S_2$ isotopologue of carbon disulfide. Data from 21 sources is extracted and validated using a consistent set of standard linear molecule quantum numbers. A corrected list of 8714 CS_2 transitions forms the input to a Measured Active Rotational–Vibrational Energy Levels (MARVEL) procedure, generating 4279 empirical rovibrational energy levels across 138 bands of $^{12}C^{32}S_2$. Results are compared to the recent NASA Ames line list. While the agreement is generally good, issues are identified with the energy levels of some states, notably those with high values of the v_2 bending quantum number.

1. Introduction

Carbon disulfide, CS_2, is a trace atmospheric species which largely comes naturally from volcanoes and from combustion, mainly due to human activity. Since 2020, CS_2 has been included in the HITRAN data base [1]. CS_2 is flammable and its spectrum is the subject of combustion studies [2]. CS_2 has been detected in comets [3,4] and the atmosphere of Jupiter following the impact of comet Shoemaker-Levy 9 [5]. Recently, CS_2 was detected in the atmosphere of Venus by the Venus Express mission [6] and evidence for CS_2 in the sub-Neptune exoplanet TOI−270 d was reported by Holmberg and Madhusudhan [7] based on observations using the James Webb Space Telescope (JWST). As discussed in detail below, $^{12}C^{32}S_2$, and indeed its various isotopologues, have been extensively characterized in the laboratory using high resolution spectroscopy [8–28]. CS_2 has also been the subject of a recent global effective Hamiltonian analysis [29] and a room-temperature, variational-nuclear-motion line list [30].

In this paper we perform a comprehensive MARVEL (Measured Active Rotational–Vibrational Energy Levels) study of $^{12}C^{32}S_2$. The MARVEL methodology has already been successfully used for OCS [31] and is being actively applied to parent CO_2 ($^{12}C^{16}O_2$) [32] alongside its various isotopologues [33–35]. There are number of advantages of these studies, not least is the large increase in the number of transitions whose line frequencies are known to experimental accuracy at the end of the procedure [36,37]. In the case of OCS, the MARVEL study [31] was used by the ExoMol project [38,39] to construct a new line list for hot OCS [40] which has very recently been used to tentatively identify the signature of OCS in the atmosphere of hot Jupiter WASP-15b using the James Webb Space Telescope [41]. The purpose of the current study is to provide the energy level input needed for the construction of the first high-temperature line list for CS_2 as part of the ExoMol project.

2. Method

2.1. The MARVEL procedure

The MARVEL algorithm [42–44] is based on the theory of spectroscopic networks (SNs) [45]. A molecular SN is described by a graph $G(E, f)$ with the nodes E being the set of energy levels and the edges f the set of transitions. On an input of the set f, MARVEL will generate the set E. The MARVEL procedure is carried out as follows:

1. Experimentally measured transitions are extracted from various sources and compiled in a grand database. This includes the experimentally derived uncertainties and unique quantum number labels associated with each transition.
2. Each transition from the cleaned database is given a tag detailing its source, and its numerical position within the source.
3. A spectroscopic network is established based on the input grand database.
4. The sources are critically evaluated for inconsistencies and mislabeling in transitions collected from different sources. An attempt is made to correctly reassign the quantum numbers of the transition if the error is obvious to spot.
5. Some data sources mention lines poorly determined by experiment. In the case of such labeled ‘weak’ or ‘blended’ lines, the uncertainty is systematically increased.
6. Transitions that do not validate are retained in the compilation but given a negative frequency and not considered by MARVEL. Their possible re-inclusion is reviewed as the final step in the

* Corresponding author.
E-mail address: j.tennyson@ucl.ac.uk (J. Tennyson).

https://doi.org/10.1016/j.jms.2025.111998
Received 14 November 2024; Received in revised form 14 January 2025; Accepted 30 January 2025
Available online 25 February 2025

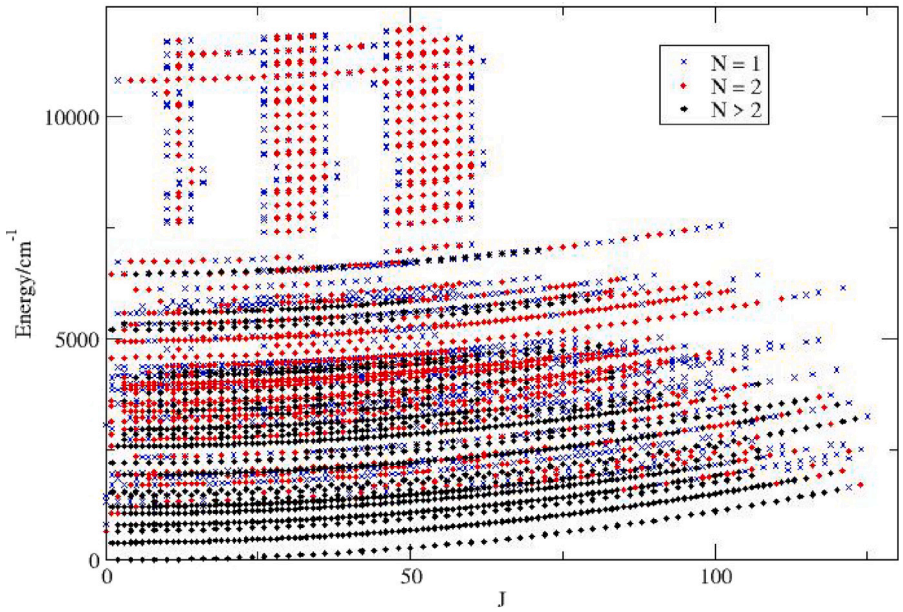

Fig. 1. Summary of $^{12}C^{32}S_2$ energy levels determined in this work designated by J and the number of transitions, N, determining them.

MARVEL process which can be done automatically using the revive facility in MARVEL4.

7. MARVEL sets up a vector of transitions within the spectroscopic network and carries out a matrix inversion to obtain the vector of energy levels.
8. Experimental uncertainties are incorporated into the calculation. The treatment of uncertainties in MARVEL has varied between the versions. The latest version, MARVEL4 [31,46,47], used here employs a bootstrap method for assigning uncertainties to the elements of the energy level vector.

2.2. Uncertainty - the bootstrap method

Questions can be asked regarding the validity of experimentally prescribed transition line uncertainties, and how these might translate to uncertainties in the empirical energy levels. The reported accuracy of high resolution spectroscopic experiments, and the subsequent determination of the associated MARVEL energy level accuracies, must be considered with care. Initial uncertainties were estimated using a variant of Watson's relatively robust weighting [48] with final results being based on bootstrap values.

MARVEL4 utilizes a bootstrap method to derive a final uncertainty for each empirical rovibrational energy levels [46]. Each transition uncertainty is scaled by a random number between 1 and 10, and MARVEL4 is run for a fixed number of iterations. If the average of the bootstrapped energies differs by a statistically significant amount from the original MARVEL energy, or the standard deviation of the bootstrapped energies is larger than the original MARVEL energy uncertainty, MARVEL4 increases the uncertainty for this energy level. A more thorough discussion is given as part of the MARVEL investigation of N_2O [46], which compares the bootstrap method to the previous method.

Previous MARVEL studies using the bootstrap method have suggested that the uncertainties generated are fairly insensitive to changes beyond 100 iterations [46] — this has therefore been used for the CS_2 project. We note that the MARVEL input format has two uncertainty columns: the first column is the original or input uncertainty. MARVEL can change (increase) the uncertainty in which case this revised value is entered in the second column; this option was not used here.

2.3. Quantum numbers and selection rules

Unlike CO_2, the rovibrational states of CS_2 are generally characterized by the standard linear-molecule, harmonic oscillator (HO) notation. Four quantum numbers are used to denote the vibrational states. v_1 and v_3 correspond to the molecule's symmetric and antisymmetric stretch respectively, and v_2 describes the degenerate bending mode. An angular momentum arises due to the bend occurring in two orthogonal planes with different phases as if the excited molecule is rotating about the molecular axis. The angular momentum quantum number ℓ takes non-negative values $v_2, v_2-2, v_2-4, \ldots$ 1 or 0. The vibrational state of the molecule can be grouped as (v_1, v_2^{ℓ}, v_3); denoted below as $(v_1\ v_2\ \ell\ v_3)$.

The quantum number J describes the molecule's rotation, with $J \geq \ell$. Additionally, there is a rotationless parity p associated with each quantum state, holding values $p = 0$ ("e" state) or $p = 1$ ("f" state) [49]. As ^{12}C and ^{32}S both have zero nuclear spin meaning that $^{12}C^{32}S_2$ has no hyperfine splittings, and that J and p are exact quantum numbers, in contrast to the approximate vibrational quantum numbers. They follow a set of strict dipole selection rules, outlined as follows: $\Delta J = 0, \pm 1$ $\Delta J = 0, e \leftrightarrow f$, but with $J = 0 \rightarrow 0$ not allowed $\Delta J = \pm 1, e \leftrightarrow e, f \leftrightarrow f$.

States with $\ell = 0$ always have a rotationless parity e, and in principle, states with $\ell \geq 1$ can have both e and f parity. In the case of symmetric CS_2, however, the Pauli principle leads to a constraint on the rotational levels which means that half of them are missing: to be present, the sum $(J+\ell+v_3+p)$ must be even. In most papers considered here, the p quantum number was not specified; the above convention was used to label and verify line assignments.

3. Results

8775 transition lines were extracted from 21 literature sources. Table 1 gives an extract of the MARVEL input file in format used by MARVEL3 [44] and MARVEL4 [46]. The full file is given in the supplementary material.

Table 2 lists the experimental sources used to construct the CS_2 rovibrational SN of this study. The data given includes, for each source, the wavenumber ranges of the validated transitions (in cm^{-1}), the number of actual versus validated (A/V) transitions, and selected uncertainty statistics (in cm^{-1}), where AOU is the average original uncertainty, AMR is the average MARVEL reproduction of the source's lines, and

Table 1
Extract from the $^{12}C^{32}S_2$ MARVEL input file. Transition wavenumbers (ν) and uncertainties (unc) are given in the units specified by the segment file. The full transitions file and the segment file are given as supplementary material.

ν	unc	unc	v_1'	v_2'	ℓ'	v_3'	p'	J'	v_1''	v_2''	ℓ''	v_3''	p''	$J\varepsilon$	tag
2185.030036	0.000010	0.000010	1	0	0	1	e	1	0	0	0	0	e	2	20KaGoKoMu.01
2184.584939	0.000010	0.000010	1	0	0	1	e	3	0	0	0	0	e	4	20KaGoKoMu.02
2184.132785	0.000010	0.000010	1	0	0	1	e	5	0	0	0	0	e	6	20KaGoKoMu.03
2183.673771	0.000010	0.000010	1	0	0	1	e	7	0	0	0	0	e	8	20KaGoKoMu.04
2183.207862	0.000010	0.000010	1	0	0	1	e	9	0	0	0	0	e	10	20KaGoKoMu.05
2182.735023	0.000010	0.000010	1	0	0	1	e	11	0	0	0	0	e	12	20KaGoKoMu.06
2182.255285	0.000010	0.000010	1	0	0	1	e	13	0	0	0	0	e	14	20KaGoKoMu.07
2181.768607	0.000010	0.000010	1	0	0	1	e	15	0	0	0	0	e	16	20KaGoKoMu.08
2181.275034	0.000010	0.000010	1	0	0	1	e	17	0	0	0	0	e	18	20KaGoKoMu.09
2180.774543	0.000010	0.000010	1	0	0	1	e	19	0	0	0	0	e	20	20KaGoKoMu.10
2180.267154	0.000010	0.000010	1	0	0	1	e	21	0	0	0	0	e	22	20KaGoKoMu.11
2179.752889	0.000010	0.000010	1	0	0	1	e	23	0	0	0	0	e	24	20KaGoKoMu.12

Table 2
$^{12}C^{32}S_2$ experimental sources used to construct the MARVEL spectroscopic network; also given are the range of transition frequencies in each source, the actual versus validated (A/V) number of transitions and the average original uncertainty (AOU), average MARVEL reproduction (AMR) of the source's lines, and maximum reproduction (MR) in the source.

Tag	Range in cm^{-1}	A/V	AOU	AMR	MR
00BlWaBrDu [11]	3083.12420 – 3168.28350	760/749	2.166e−04	1.702e−04	0.786
01BlWaBrDu [21]	3402.60150 – 4242.43020	1122/1122	3.000e−04	1.952e−04	0.651
04HoAnPiAl [22]	240.55342 – 1236.83693	607/593	1.195e−04	1.471e−04	1.231
12VaTsLeHe [9]	6097.02420 – 6466.26510	198/198	1.036e−02	8.070e−03	0.779
20KaGoKoMu [8]	2140.27362 – 2198.93869	688/688	1.000e−05	9.085e−06	0.909
70SmOv [23]	1512.74500 – 1549.85800	175/166	1.524e−03	5.495e−03	3.606
71SmOv [10]	378.87400 – 412.33200	70/69	3.000e−03	1.089e−02	3.629
73Maki [13]	2286.36930 – 2977.04550	314/312	2.000e−03	1.261e−03	0.631
74MaSa [24]	2125.25720 – 2198.89730	511/502	1.181e−03	2.296e−03	1.944
79JoKaAn [14]	245.39500 – 275.65770	97/97	2.000e−04	4.716e−04	2.358
80JoKa [25]	368.71100 – 430.26260	551/536	6.000e−04	1.415e−03	2.358
84BaBlWaCo [15]	842.50650 – 894.92090	462/433	1.005e−03	7.301e−04	0.727
85BlBaCaWa [16]	842.74040 – 892.89450	353/299	5.000e−04	1.965e−04	0.393
85LiJo [17]	1492.22240 – 1561.74990	289/261	2.000e−04	2.549e−04	1.275
86DaBlWaCo [27]	857.04020 – 893.80860	56/56	1.000e−03	6.194e−04	0.619
88WeScMa [26]	1500.60364 – 1549.03823	7/7	1.239e−04	1.232e−04	0.995
92BlWaBlBr [18]	4489.59360 – 4572.26230	682/681	3.000e−04	1.656e−04	0.552
92WaMaBl [19]	689.69200 – 744.37560	246/245	4.000e−04	4.380e−04	1.095
96PlMaHoDe [12]	6438.74600 – 6466.42300	58/56	5.000e−03	5.294e−03	1.059
99BlWaBrDu [20]	5139.23960 – 5337.35300	309/309	4.000e−04	2.778e−04	0.695
99LiHu [28]	3302.78700 – 11995.63900	1220/1220	1.000e−01	4.882e−02	0.488

MR the maximum reproduction in the source. We note that in the A/V statistic, the validated number refers solely to transitions in the main network and components in the sub networks are not counted. Of the 8775 original considered, 53 had to be removed as this were not validated by the MARVEL procedure. The remaining data contained 7430 unique transitions. Notes on our use of these experimental sources are provided in Appendix A.

The main MARVEL SN contained 8599 transitions. A total of 4279 energy levels were given by the main network. Energy levels which are characterized by many transitions are both secure and well-determined. Table 3 gives an extract of the energy file produced by the MARVEL procedure; the full file is given in the supplementary material. The uncertainties in this file are given by running the bootstrap procedure 100 times during the final MARVEL run. These uncertainties are generally slightly higher than those given initially by MARVEL and summarized in Table 2; this is probably reflection of slightly optimistic estimation of uncertainties in some of the experimental studies. We note that the bootstrap procedure does not alter the uncertainties associated with levels determined by a single transition, suggesting that these uncertainties may be underestimated.

Fig. 1 plots the energy levels as function of J and energy; the plot distinguishes between levels which are linked by only one transition ($N = 1$), two ($N = 2$) and many ($N > 2$) transitions. In practice 1178 levels are characterized by a single transition, 1658 by two transitions and 1443 by more (in some cases more than 40) transitions. While levels characterized by only one transition cannot be regarded as secure, the generally smooth behavior of the levels as a function of J suggests that most of these levels are indeed correctly characterized.

Table 3
Extract from the $^{12}C^{32}S_2$ energy levels output file giving standard quantum numbers, energies with associated bootstrap uncertainty (100 iterations), plus the number of transitions (N) associated with each level. The full file is given as supplementary material.

v_1	v_2	ℓ	v_3	p	J	E/cm^{-1}	unc/cm^{-1}	N
0	0	0	0	e	0	0.000000000	0.0	1233
0	0	0	0	e	2	0.654706804	1.862e−05	25
0	0	0	0	e	4	2.182361347	3.436e−05	29
0	0	0	0	e	6	4.583103085	5.137e−05	36
0	0	0	0	e	8	7.856854164	6.889e−05	42
0	0	0	0	e	10	12.003562632	9.015e−05	43
0	0	0	0	e	12	17.023231708	1.146e−04	44
0	0	0	0	e	14	22.915814696	1.388e−04	46
0	0	0	0	e	16	29.681277718	1.604e−04	44
0	0	0	0	e	18	37.319587303	1.792e−04	44
0	0	0	0	e	20	45.830710347	1.992e−04	46
0	0	0	0	e	22	55.214615363	2.186e−04	46

3.1. Comparison with NASA Ames line list

The NASA Ames $^{12}C^{32}S_2$ line list [30] contains 1 856 648 $^{12}C^{32}S_2$ rovibrational lines and covers the 0 - 6909 cm^{-1}wavenumber region. These transitions were generated using variational nuclear motion calculation with many of the energy levels replaced by the results of an Effective Hamiltonian model calculation [29]. 3494 of the 4279 levels (66 of the 138 vibrational bands) underwent comparison; results of this comparison can be seen in Figs. 2–4. Most of the vibrational bands not

Table 4
Table of energy levels with low v_2 and with residues between MARVEL/Ames lists greater than 0.01cm^{-1}.

N	E(Ames)/cm^{-1}	E(MARVEL)/cm^{-1}	unc(MARVEL)/cm^{-1}	v_1	v_2	ℓ	v_3	J	Obs(MARVEL) - Calc(Ames)/cm^{-1}
2	1592.55085	1591.551616	0.001316	0	2	2	0	85	−0.99923
3	2477.47641	2477.457898	0.001439	0	2	0	1	37	−0.01851
1	3042.57405	3042.062948	0.003235	1	3	1	0	104	−0.51110
1	3088.72932	3088.715280	0.00327	1	3	1	0	106	−0.01404
1	3344.33572	3344.325423	0.002219	0	3	1	1	75	−0.01030
2	3632.40270	3632.324842	0.003949	1	3	1	1	50	−0.07786
1	3726.39141	3725.388616	0.002471	1	2	2	1	84	−1.00279
1	3766.90884	3766.919275	0.002147	1	3	1	1	61	0.01044
1	3794.08654	3794.166824	0.002155	1	3	1	1	63	0.08028
2	3880.94415	3880.933889	0.002195	1	3	1	1	69	−0.01026
1	3900.24745	3900.233803	0.002987	1	2	2	1	93	−0.01364
1	3998.73622	3998.99	0.1	6	0	0	0	28	0.25
1	4025.89849	4025.882898	0.002719	1	2	2	1	99	−0.01559
1	4163.10950	4163.021	0.1	3	6	2	0	14	−0.088
4	6554.57906	6554.565344	0.01365	3	0	0	3	29	−0.01372
3	6628.10881	6628.120680079	0.005015	3	0	0	3	39	0.01187

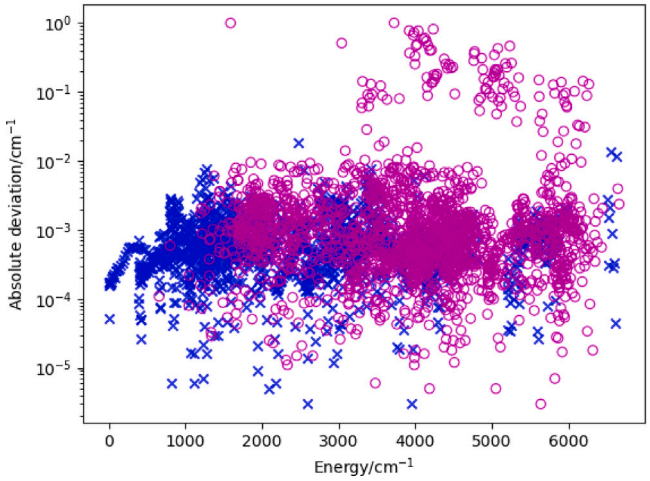

Fig. 2. Plot of absolute residues between MARVEL/Ames lines against the associated MARVEL energy. Blue crosses represent levels associated with 3 or more transitions; magenta circles represent levels with 2 or less transitions.

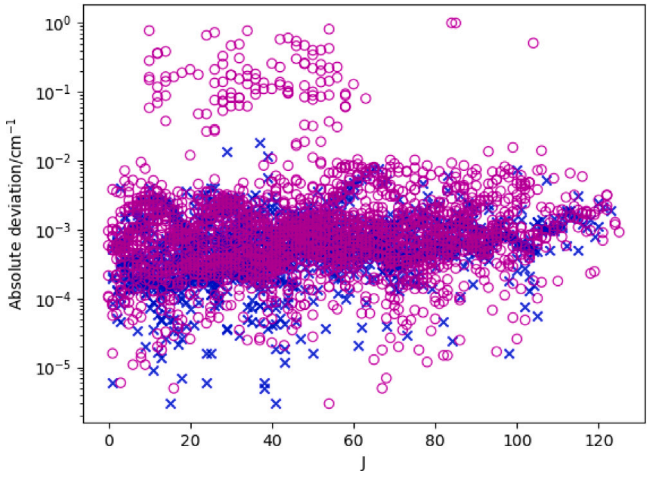

Fig. 3. Absolute residues between MARVEL/Ames lines are plotted against the associated J value. Blue crosses represent levels associated with 3 or more transitions; magenta circles represent levels with 2 or less transitions.

analyzed have band centers above the NASA Ames wavenumber range. However, three lower-lying bands, (0 4 0 3), (2 2 0 3) and (0 1 1 4), could not be verified by the Ames line list either. This is likely due

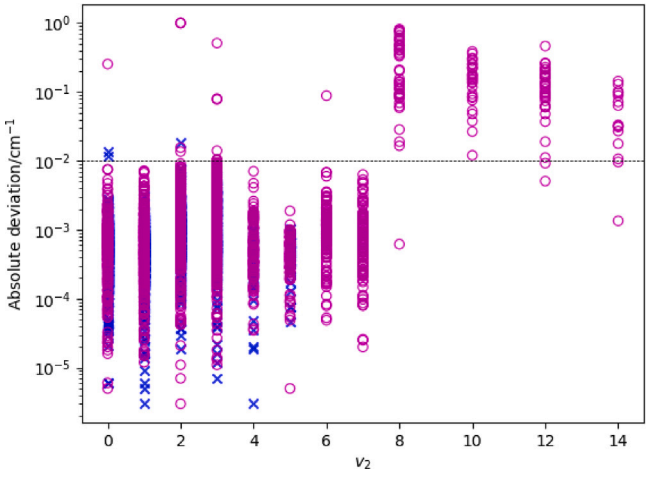

Fig. 4. Plot of absolute differences against the associated v_2 quantum number. Blue crosses represent levels associated with 3 or more transitions; magenta circles represent levels with 2 or less transitions. Generally states with high values of v_2 seem to carry greatest differences.

to issues with quantum number labeling and that these bands are not included in Tashkun's effective Hamiltonian model. Almost all of the differences are smaller than 0.01 cm^{-1}; the deviations are larger than 0.01 cm^{-1} only for relatively high v_2 values.

A comparison of the mean and standard deviations of the residues for low and high v_2 states is given i in Table 5. There is a marked difference between levels with $v_2 < 8$ and $v_2 \geq 8$. The standard deviation is bigger by one order of magnitude for high v_2 levels, and the mean is increased by approximately 2 orders of magnitude.

On checking how many experimental measurements determine the MARVEL energy levels that have a large difference from the values, most of them are determined by only one or two measurements (see the magenta circle markers in Figs. 2 and 4). While MARVEL levels determined by a single measurement are regarded as less trustworthy, the systematic correlation of high absolute deviations with high v_2 values suggests high v_2 states are not well represented in the Ames line list. A full list of levels which differ by more than 0.01 cm^{-1} between MARVEL and Ames is provided in the supplementary material; Table 4 provides a list of low v_2 levels which differ by more than 0.01 cm^{-1}.

Effective Hamiltonians can be an extremely effective and accurate method for representing experimental data. In favorable cases they can even improve on the uncertainty of individual measurements and can interpolate reliably between measured levels. However, resonances, where levels from different vibrational bands with the same overall

Table 5
Comparison of MARVEL and Ames energy levels for low and high v_2 levels: standard deviation of signed deviations, and mean of signed and absolute deviations.

	$v_2 < 8$	$v_2 \geq 8$
Standard deviation (Obs(MARVEL)-Calc(Ames)) cm^{-1}	0.0264	0.2413
Mean (Obs(MARVEL)-Calc(Ames)) cm^{-1}	−0.0013	−0.0927
Mean (Absolute deviation) cm^{-1}	0.0020	0.1844

symmetry interact, can be problematic. MARVEL has no difficulties with resonances in principle but requires multiple transitions to a given level for the energy to be securely determined unless there is an independent means of confirming them such as an independently computed line list. It is likely that at least some of the differences listed in Table 4 are caused by resonances which have not been fully accounted for in the effective Hamiltonian treatment.

4. Conclusion

We present a MARVEL analysis of $^{12}C^{32}S_2$ high resolution spectra which result in the determination of 4279 empirical energy levels. The uncertainties for these levels were determined by the implementation the new MARVEL4 bootstrap approach, with an iteration count of 100. Comparison of these levels with a recently produced NASA Ames line list [30] generally gives very good agreement but identifies highly excited bending states as needing more work to better characterize them by, for example, improving the representation the higher bending states by an *ab initio* or fitted potential energy surface (PES). We note that MARVEL provides energy levels up to ones with $v_2 = 22$, so there are plenty of levels to test against in constructing such a PES. The plan is to use the present study as the starting point to generate a hot $^{12}C^{32}S_2$ line list as part of the ExoMol project; we note that the treatment of excited bending states is particularly important for high temperatures as it is these states that give rise to many of the hot bands that are a key characteristic of hot line lists. While empirical energy levels provide important input to such a line list, experience shows that transition intensities can be computed to high accuracy using *ab initio* dipole moment surfaces [50,51].

Further MARVEL studies could also be conducted on the some of the major isotopologues of CS_2. Of particular interest for astronomy may be those molecules containing ^{13}C, due to its high relative abundance in parts of the Universe. Although a fair number of experiments have been carried out into the rovibrational spectra of these isotopologues, it is unclear whether there is enough experimental data to form a robust MARVEL spectroscopic network.

CRediT authorship contribution statement

Tanvi Sattiraju: Writing – original draft, Visualization, Validation, Investigation, Formal analysis, Data curation. **Jonathan Tennyson:** Writing – review & editing, Supervision, Methodology, Funding acquisition, Conceptualization.

Declaration of competing interest

The authors declare no conflict of interest.

Acknowledgments

TS thanks UCL's Faculty of Maths and Physics Sciences (MAPS) for the provision of summer studentship. This work was supported by ERC Advanced Investigator Project grant 883830.

Appendix A. Notes on data sources

20KaGoKoMu [8]: The uncertainty is given in the paper as 'better than 0.00001 cm^{-1}'. This is the value used for all lines.

12VaTsLeHe [9]: An uncertainty of 0.008 cm^{-1} was estimated from the standard deviation table for all lines. This was perhaps a little optimistic, as reflected in the initial MARVEL run. As a result, the uncertainties of the lines in the (0403) - (0000) band were increased to 0.026 cm^{-1}.

71SmOv [10]: The uncertainty was estimated to be 0.003 cm^{-1} for all lines. The R(60) line observed in the (0 1 1 0) - (0 0 0 0) band was removed due to inconsistency.

00BlWaBrDu [11]: An uncertainty of 0.002 cm^{-1} was assumed, estimated from the standard deviation table given. Two pairs of lines were removed due to self contradictory energy levels. The first pair consisted of the P(26) and R(24) lines in the (0 4 0 1) - (0 0 0 0) band, and the second pair was the R(86) and P(88) lines in the (0 5 1 1) - (0 1 1 0) band.

96PlMaHoDe [12]: An experimental accuracy of 0.005 cm^{-1} was provided in the paper — this was taken to be the uncertainty. The P(18) and P(20) lines observed in the (3 0 0 3) - (0 0 0 0) band were removed due to inconsistency.

73Maki [13]: An uncertainty of 0.002 cm^{-1} was assumed, estimated from the standard deviation table. Some lines were labeled as 'transitions to perturbed levels', however these uncertainties were kept the same. The R(47) line observed in the (1 3 1 1) - (0 1 1 0) band was removed due to inconsistency.

79JoKaAn [14]: An uncertainty of 0.0002 cm^{-1} was assumed, estimated from the standard deviation given for the band centres.

84BaBlWaCo [15]: The uncertainty was taken to be 0.001 cm^{-1}, as mentioned in the paper. The P(97) line observed in the (0 1 1 1) - (1 1 1 0) band was removed due to inconsistency. The uncertainties for two lines in the (0 2 0 1) - (1 2 0 0) band were doubled — these lines were both assigned J' = 37.

85BlBaCaWa [16]: An uncertainty of 0.0005 cm^{-1} was assumed, estimated from the standard deviation table given.

85LiJo [17]: An uncertainty of 0.002 cm^{-1} was assumed, estimated from the standard deviation table. The R(64) line observed in the (1 0 0 1) - (1 0 0 0) band was removed due to inconsistency.

92BlWaBlBr [18]: An uncertainty of 0.0003 cm^{-1} was assumed, estimated from the standard deviation table given.

92WaMaBl [19]: An uncertainty of 0.0004 cm^{-1} was assumed, estimated from the standard deviation table given. The R(95) line observed in the (0 1 1 1) - (0 3 1 0) band was removed due to inconsistency.

99BlWaBrDu [20]: An uncertainty of 0.0004 cm^{-1} was assumed, estimated from the standard deviation table given.

01BlWaBrDu [21]: An uncertainty of 0.0003 cm^{-1} was assumed, estimated from the standard deviation table given. The R(64) line in the (1 5 1 1) - (0 1 1 0) band was removed due to inconsistencies.

04HoAnPiAl [22]: The uncertainties, as assigned to every line, were adopted directly from the paper. These proved to be very optimistic, so every uncertainty was scaled up by a factor of 10. Four particularly bad lines plus 15 lines belonging to the (0 3 1 0) - (0 0 0 0) and (0 1 1 0) - (0 0 0 0) bands were removed due to inconsistencies.

70SmOv [23]: An uncertainty of 0.001 cm^{-1} was assumed, estimated from the standard deviation table. 9 lines belonging to the (0 0 0 1) - (0 0 0 0) band were removed due to inconsistencies.

74MaSa [24]: An uncertainty of 0.001 cm^{-1} was estimated from the standard deviation table. This was doubled for transitions labeled in

the paper as 'weak/blended'. The P(70) and R(68) lines observed in the (2 1 1 1) - (1 1 1 0) band were removed due to inconsistency. The R(50) line observed in the (1 2 2 1) - (0 2 2 0) band was also removed.

80JoKa [25]: The uncertainty was estimated to be 0.0006 cm^{-1}, from the standard deviation table. This was a little optimistic, as reflected in the MARVEL bad line analysis. The MARVEL4 bootstrap method was used to calculate improved uncertainties for the associated energy levels. 15 lines belonging to the (0 3 1 0) - (0 2 2 0), (0 3 1 0) - (0 2 0 0), (1 1 1 0) - (1 0 0 0) and (0 2 2 0) - (0 1 1 0) bands were removed due to inconsistencies while two lines were corrected for obvious typographic errors.

88WeScMa [26]: This paper contains measured transitions in MHz — the MARVEL4 segment file was updated to reflect this. The uncertainties were obtained directly from the paper for each line.

86DaBlWaCo [27]: This paper contained only spectral intensities, and raw transition data was not publicly available. However, the line positions are given in Tashkun's recent paper using an effective Hamiltonian to construct a line list [29] and the attached data file was used as a secondary source.

99LiHu [28]: This paper reports stimulated emission spectra which provide observed energy levels for both the ground and R $^3B_2$ excited states. Although the excited state vibrational bands were ambiguously assigned, there are clear data for the ground levels. The lower level of the transition was taken to be $(v_1, v_2, l, v_3, J) = (0\ 0\ 0\ 0\ 0)$ in each case. The uncertainty was set to 0.1 cm^{-1} for every line. This was taken from the data file attached to the recent paper by Tashkun [29], which used an effective Hamiltonian to model line positions for CS_2.

Appendix B. Supplementary data

MARVEL input file - MARVEL4_input_CS2_28Dec24.txt

A segment file necessary for running MARVEL4 - Marvel4_segment_CS2.txt.

MARVEL output energies file - MARVEL_EnergyLevels_28Dec24.txt

MARVEL AMES energy comparison file - Ames+MARVEL_comparison_28Dec24.txt

A file of levels differing by more than 0.01 cm^{-1} between MARVEL and the NASA Ames line list - Residues_0.01_28Dec.txt

Supplementary material related to this article can be found online at https://doi.org/10.1016/j.jms.2025.111998.

Data availability

All data is provided in the supporting material.

References

[1] I.E. Gordon, L.S. Rothman, R.J. Hargreaves, R. Hashemi, E.V. Karlovets, F.M. Skinner, E.K. Conway, C. Hill, R.V. Kochanov, Y. Tan, P. Wcisło, A.A. Finenko, K. Nelson, P.F. Bernath, M. Birk, V. Boudon, A. Campargue, K.V. Chance, A. Coustenis, B.J. Drouin, J. Flaud, R.R. Gamache, J.T. Hodges, D. Jacquemart, E.J. Mlawer, A.V. Nikitin, V.I. Perevalov, M. Rotger, J. Tennyson, G.C. Toon, H. Tran, V.G. Tyuterev, E.M. Adkins, A. Baker, A. Barbe, E. Canè, A.G. Császár, A. Dudaryonok, O. Egorov, A.J. Fleisher, H. Fleurbaey, A. Foltynowicz, T. Furtenbacher, J.J. Harrison, J. Hartmann, V. Horneman, X. Huang, T. Karman, J. Karns, S. Kassi, I. Kleiner, V. Kofman, F. Kwabia-Tchana, N.N. Lavrentieva, T.J. Lee, D.A. Long, A.A. Lukashevskaya, O.M. Lyulin, V.Y. Makhnev, W. Matt, S.T. Massie, M. Melosso, S.N. Mikhailenko, D. Mondelain, H.S.P. Müller, O.V. Naumenko, A. Perrin, O.L. Polyansky, E. Raddaoui, P.L. Raston, Z.D. Reed, M. Rey, C. Richard, R. Tóbiás, I. Sadiek, D.W. Schwenke, E. Starikova, K. Sung, F. Tamassia, S.A. Tashkun, J. Vander Auwera, I.A. Vasilenko, A.A. Vigasin, G.L. Villanueva, B. Vispoel, G. Wagner, A. Yachmenev, S.N. Yurchenko, The HITRAN2020 molecular spectroscopic database, J. Quant. Spectrosc. Radiat. Transfer 277 (2020) 107949, http://dx.doi.org/10.1016/j.jqsrt.2021.107949.

[2] W. d. Peng, J. l. Ning, Z. l. Chen, J. Tang, L. x. Liu, L. Chen, Construction of CS_2 combustion flame spectral radiation model and inversion of characteristic pollution product concentration, Spectrosc. Spectal Anal. 42 (2022) 672–677, http://dx.doi.org/10.3964/j.issn.1000-0593(2022)03-0672-06.

[3] W.M. Jackson, A. Scodinu, D. Xu, A.L. Cochran, Using the ultraviolet and visible spectrum of comet 122P/de Vico to identify the parent molecule CS2, Astrophys. J. 607 (2004) L139–L141, http://dx.doi.org/10.1086/421995.

[4] U. Calmonte, K. Altwegg, H. Balsiger, J.J. Berthelier, A. Bieler, G. Cessateur, F. Dhooghe, E.F. van Dishoeck, B. Fiethe, S.A. Fuselier, S. Gasc, T.I. Gombosi, M. Hässig, L. Le Roy, M. Rubin, T. Sémon, C.-Y. Tzou, S.F. Wampfler, Sulphur-bearing species in the coma of comet 67P/Churyumov–Gerasimenko, Mon. Not. R. Astron. Soc. 462 (2016) S253–S273, http://dx.doi.org/10.1093/mnras/stw2601.

[5] S.K. Atreya, S.G. Edgington, L.M. Trafton, J.J. Caldwell, K.S. Noll, H.A. Weaver, Abundances of ammonia and carbon disulfide in the Jovian stratosphere following the impact of comet Shoemaker-Levy 9, Geophys. Res. Lett. 22 (1995) 1625–1628, http://dx.doi.org/10.1029/95GL01718.

[6] A. Mahieux, S. Robert, F.P. Mills, K.L. Jessup, L. Trompet, S. Aoki, A. Piccialli, J. Peralta, A.C. Vandaele, Update on SO_2, detection of OCS, CS, CS_2, and SO_3, and upper limits of H_2S and HOCl in the Venus mesosphere using SOIR on board Venus Express, ICARUS 399 (2023) 115556, http://dx.doi.org/10.1016/j.icarus.2023.115556.

[7] M. Holmberg, N. Madhusudhan, Possible Hycean conditions in the sub-Neptune TOI-270 d, Astron. Astrophys. 683 (2024) L2, http://dx.doi.org/10.1051/0004-6361/202348238.

[8] E.V. Karlovets, I.E. Gordon, D. Konnov, A.V. Muraviev, K.L. Vodopyanov, Dual-comb laser spectroscopy of CS_2 near 4.6 μm, J. Quant. Spectrosc. Radiat. Transfer 256 (2020) 107269, http://dx.doi.org/10.1016/j.jqsrt.2020.107269.

[9] X. de Ghellinck d'Elseghem Vaernewijck, P. Kongolo Tshikala, M. Lepère, M. Herman, Femto-FT-CEAS applied to Carbon Disulfide around 1.54 μm, J. Mol. Spectrosc. 282 (2012) 27–29, http://dx.doi.org/10.1016/j.jms.2012.10.006.

[10] D.F. Smith Jr., J. Overend, General quartic force field of CS_2, J. Chem. Phys. 54 (1971) 3632–3639, http://dx.doi.org/10.1063/1.1675389.

[11] G. Blanquet, J. Walrand, H. Bredohl, I. Dubois, Fourier transform infrared spectrum of Carbon Disulphide in the $4\nu_2+\nu_3$ band region near 3100 cm^{-1}, Mol. Phys. 98 (2000) 2021–2031, http://dx.doi.org/10.1080/00268970009483405.

[12] T. Platz, M. Matheis, C. Hornberger, W. Demtröder, High-sensitivity overtone spectroscopy of carbon disulfide CS_2, J. Mol. Spectrosc. 180 (1996) 81–84, http://dx.doi.org/10.1006/jmsp.1996.0226.

[13] A.G. Maki, Infrared spectra of CS_2: Measurement of hot bands associated with the 2325 cm^{-1} and 2962 cm^{-1} bands, J. Mol. Spectrosc. 47 (2) (1973) 217–225, http://dx.doi.org/10.1016/0022-2852(73)90005-2.

[14] K. Jolma, J. Kauppinen, R. Anttila, The difference band $\nu_1 - \nu_2$ of $^{12}C^{32}S_2$, J. Chem. Phys. 70 (1979) 2033–2034, http://dx.doi.org/10.1063/1.437639.

[15] E. Baeten, G. Blanquet, J. Walrand, C.P. Courtoy, Tunable diode laser spectra of the $\nu_3 - \nu_1$ region of CS_2, Can. J. Phys. 62 (1984) 1286–1292, http://dx.doi.org/10.1139/p84-174.

[16] G. Blanquet, E. Baeten, I. Cauuet, J. Walrand, C.P. Courtoy, Diode-laser measurements of Carbon Disulfide and general rovibrational analysis, J. Mol. Spectrosc. 112 (1985) 55–70, http://dx.doi.org/10.1016/0022-2852(85)90191-2.

[17] J. Lindenmayer, H. Jones, Diode laser spectroscopy of the ν_3 band region of four isotopic forms of CS_2, J. Mol. Spectrosc. 110 (1985) 65–73, http://dx.doi.org/10.1016/0022-2852(85)90212-7.

[18] G. Blanquet, J. Walrand, J.-F. Blavier, H. Bredohl, I. Dubois, Fourier transform infrared spectrum of CS_2: Analysis of the $3\nu_3$ band, J. Mol. Spectrosc. 152 (1992) 137–151, http://dx.doi.org/10.1016/0022-2852(92)90124-7.

[19] J. Walrand, P. Maree, G. Blanquet, Diode-laser spectrum of Carbon Disulfide CS_2 in the region of 13.6 μm, J. Mol. Spectrosc. 155 (1992) 158–166, http://dx.doi.org/10.1016/0022-2852(92)90555-3.

[20] G. Blanquet, J. Walrand, H. Bredohl, I. Dubois, High-resolution spectra of Carbon Disulfide $^{12}C^{32}S_2$ in the region of 2 μm, J. Mol. Spectrosc. 198 (1999) 43–51, http://dx.doi.org/10.1006/jmsp.1999.7932.

[21] G. Blanquet, J. Walrand, H. Bredohl, I. Dubois, Spectra of Carbon Disulphide in the 3400–4400 cm^{-1} region by Fourier transform spectroscopy, Mol. Phys. 99 (2001) 1469–1484, http://dx.doi.org/10.1080/00268970110060811.

[22] V.-M. Horneman, R. Anttila, J. Pietilä, S. Alanko, M. Koivusaari, Transferring the high accuracy of the 10 μm CO_2 laser bands to far infrared region with internal calibration of CS_2, J. Mol. Spectrosc. 229 (2005) 89–107, http://dx.doi.org/10.1016/j.jms.2004.08.016.

[23] D.F. Smith, J. Overend, The ν_3 bands of $^{12}C^{32}S_2$ and $^{13}C^{32}S_2$ at high resolution, Spectrochim. Acta Part A: Mol. Spectrosc. 26 (1970) 2269–2274, http://dx.doi.org/10.1016/0584-8539(70)80178-7.

[24] A.G. Maki, R.L. Sams, Infrared spectrum of CS_2: Hot bands associated with the 2185 cm^{-1} band and evidence for the CS_2 laser assignment, J. Mol. Spectrosc. 52 (1974) 233–243, http://dx.doi.org/10.1016/0022-2852(74)90114-3.

[25] K. Jolma, J. Kauppinen, High-resolution infrared spectrum of CS_2 in the region of the bending fundamental ν_2, J. Mol. Spectrosc. 82 (1980) 214–219, http://dx.doi.org/10.1016/0022-2852(80)90111-3.

[26] J.S. Wells, M. Schneider, A.G. Maki, Calibration tables covering the 1460 to 1550 cm^{-1} region from heterodyne frequency measurements on the ν_3 bands of $^{12}CS_2$ and $^{13}CS_2$, J. Mol. Spectrosc. 132 (1988) 422–428, http://dx.doi.org/10.1016/0022-2852(88)90337-2.

[27] M. Dang-Nhu, G. Blanquet, J. Walrand, C.P. Courtoy, Spectral intensities in the $\nu_3 - \nu_1$ band of CS_2, Mol. Phys. 58 (1986) 995–1000, http://dx.doi.org/10.1080/00268978600101741.

[28] H.T. Liou, K.L. Huang, Fermi-resonances, potential energy function, and cluster-like spectra of the ground electronic state of CS_2, Chem. Phys. 246 (1999) 391–431, http://dx.doi.org/10.1016/S0301-0104(99)00189-5.

[29] S.A. Tashkun, Global modeling of the $^{12}C^{32}S_2$ line positions within the framework of the non-polyad model of effective Hamiltonian, J. Quant. Spectrosc. Radiat. Transfer 279 (2022) 108072, http://dx.doi.org/10.1016/j.jqsrt.2022.108072.

[30] X. Huang, I.E. Gordon, S.A. Tashkun, D.W. Schwenke, T.J. Lee, Accurate infrared line lists for 20 isotopologues of CS_2 at room temperature, Astrophys. J. Suppl. Ser. 272 (2024) 17, http://dx.doi.org/10.3847/1538-4365/ad3809.

[31] E. Xu, J. Tennyson, Empirical rovibrational energy levels for carbonyl sulphide, Mol. Phys. 122 (2024) e2279694, http://dx.doi.org/10.1080/00268976.2023.2279694.

[32] A.A.A. Azzam, B.M.J. Abou Doud, M.Q.A. Shersheer, B.K.M. Almasri, C.N.M. Bader, A.M.H.A. Baraa, O.A.K.H. Musleh, A.W.M. Al Shatarat, B.I.M. Qattan, L.H.M. Hamamsy, A.O.G. Saafneh, M.N.A. ALso'ub, M.M.A. Alkhashashneh, H.O.M. Al-Zawahra, D. Alatoom, M.T.I. Ibrahim, J. Tennyson, S.N. Yurchenko, T. Furtenbacher, A.G. Császár, MARVEL analysis of high-resolution rovibrational spectra of $^{16}O^{12}C^{16}O$, Sci. Data.

[33] M.T.I. Ibrahim, D. Alatoom, T. Furtenbacher, A.G. Császár, S.N. Yurchenko, A.A.A. Azzam, J. Tennyson, MARVEL analysis of high-resolution rovibrational spectra of $^{13}C^{16}O_2$, J. Comput. Chem. 45 (2024) 969–984, http://dx.doi.org/10.1002/jcc.27266.

[34] D. Alatoom, M.T.I. Ibrahim, T. Furtenbacher, A.G. Császár, M. Alghizzawi, S.N. Yurchenko, A.A.A. Azzam, J. Tennyson, MARVEL analysis of high-resolution rovibrational spectra of $^{16}O^{12}C^{18}O$, J. Comput. Chem. 45 (2024) 2558, http://dx.doi.org/10.1002/jcc.27453.

[35] A.A.A. Azzam, S.A.A. Azzam, K.A.A. Aburumman, J. Tennyson, S.N. Yurchenko, A.G. Császár, T. Furtenbacher, MARVEL analysis of high-resolution rovibrational spectra of $^{18}O^{12}C^{18}O^{17}O^{12}C^{18}O$ and $^{18}O^{13}C^{18}O$ isotopologues of carbon dioxide, J. Mol. Spectrosc. 405 (2024) 111947, http://dx.doi.org/10.1016/j.jms.2024.111947.

[36] A.R. Al-Derzi, S.N. Yurchenko, J. Tennyson, M. Melosso, N. Jiang, C. Puzzarini, L. Dore, T. Furtenbacher, R. Tobias, A.G. Császár, An improved rovibrational linelist of formaldehyde $H_2^{12}C^{16}O$, J. Quant. Spectrosc. Radiat. Transfer 266 (2021) 107563, http://dx.doi.org/10.1016/j.jqsrt.2021.107563.

[37] C.A. Bowesman, Q. Qu, L.K. McKemmish, S.N. Yurchenko, J. Tennyson, ExoMol line lists – LV: Hyperfine-resolved molecular line list for vanadium monoxide ($^{51}V^{16}O$), Mon. Not. R. Astron. Soc. 529 (2024) 1321–1332, http://dx.doi.org/10.1093/mnras/stae542.

[38] J. Tennyson, S.N. Yurchenko, ExoMol: molecular line lists for exoplanet and other atmospheres, Mon. Not. Roy. Astron. Soc. 425 (2012) 21–33, http://dx.doi.org/10.1111/j.1365-2966.2012.21440.x.

[39] J. Tennyson, S.N. Yurchenko, J. Zhang, C.A. Bowesman, R.P. Brady, J. Buldyreva, K.L. Chubb, R.R. Gamache, M.N. Gorman, E.R. Guest, C. Hill, K. Kefala, A.E. Lynas-Gray, T.M. Mellor, L.K. McKemmish, G.B. Mitev, I.I. Mizus, A. Owens, Z. Peng, A.N. Perri, M. Pezzella, O.L. Polyansky, Q. Qu, M. Semenov, O. Smola, A. Solokov, W. Somogyi, A. Upadhyay, S.O.M. Wright, N.F. Zobov, The 2024 release of the ExoMol database: molecular line lists for exoplanet and other hot atmospheres, J. Quant. Spectrosc. Radiat. Transfer 326 (2024) 109083, http://dx.doi.org/10.1016/j.jqsrt.2024.109083.

[40] A. Owens, S.N. Yurchenko, J. Tennyson, ExoMol line lists - LVIII. High-temperature molecular line list of carbonyl sulphide (OCS), Mon. Not. Roy. Astron. Soc. 530 (2024) 4004–4015, http://dx.doi.org/10.1093/mnras/stae1110.

[41] J. Kirk, E.-M. Ahrer, A.B. Claringbold, M. Zamyatina, C. Fisher, M. McCormack, V. Panwar, D. Powell, J. Taylor, D.P. Thorngren, D.A. Christie, E. Esparza-Borges, S.-M. Tsai, L. Alderson, R.A. Booth, C. Fairman, M. López-Morales, N.J. Mayne, A. Meech, P. Molliere, J.E. Owen, A.B.T. Penzlin, D.E. Sergeev, D. Valentine, H.R. Wakeford, P.J. Wheatley, BOWIE-ALIGN: JWST reveals hints of planetesimal accretion and complex sulphur chemistry in the atmosphere of the misaligned hot Jupiter WASP-15b, Mon. Not. Roy. Astron. Soc. 537 (2025) 3027–3052, http://dx.doi.org/10.1093/mnras/staf208.

[42] T. Furtenbacher, A.G. Császár, J. Tennyson, MARVEL: measured active rotational-vibrational energy levels, J. Mol. Spectrosc. 245 (2007) 115–125, http://dx.doi.org/10.1016/j.jms.2007.07.005.

[43] T. Furtenbacher, T. Szidarovszky, E. Mátyus, C. Fábri, A.G. Császár, Analysis of the rotational–vibrational states of the molecular ion H_3^+, J. Chem. Theory Comput. 9 (2013) 5471–5478, http://dx.doi.org/10.1021/ct4004355.

[44] R. Tóbiás, T. Furtenbacher, J. Tennyson, A.G. Császár, Accurate empirical rovibrational energies and transitions of $H_2^{16}O$, Phys. Chem. Chem. Phys. 21 (2019) 3473–3495, http://dx.doi.org/10.1039/c8cp05169k.

[45] A.G. Császár, T. Furtenbacher, Spectroscopic networks, J. Mol. Spectrosc. 266 (2011) 99–103, http://dx.doi.org/10.1016/j.jms.2011.03.031.

[46] J. Tennyson, T. Furtenbacher, S.N. Yurchenko, A.G. Császár, Empirical rovibrational energy levels for nitrous oxide, J. Quant. Spectrosc. Radiat. Transfer 316 (2024) 108902, http://dx.doi.org/10.1016/j.jqsrt.2024.108902.

[47] J. Tennyson, Empirical rovibronic energy levels of C_3, Mol. Phys. 122 (2024) e2276912, http://dx.doi.org/10.1080/00268976.2023.2276912.

[48] J.K.G. Watson, Robust weighting in least-squares fits, J. Mol. Spectrosc. 219 (2003) 326–328, http://dx.doi.org/10.1016/S0022-2852(03)00100-0.

[49] J.M. Brown, J.T. Hougen, K.-P. Huber, J.W.C. Johns, I. Kopp, H. Lefebvre-Brion, A.J. Merer, D.A. Ramsay, J. Rostas, R.N. Zare, The labeling of parity doublet levels in linear molecules, J. Mol. Spectrosc. 55 (1975) 500–503, http://dx.doi.org/10.1016/0022-2852(75)90291-X.

[50] O.L. Polyansky, K. Bielska, M. Ghysels, L. Lodi, N.F. Zobov, J.T. Hodges, J. Tennyson, High accuracy CO_2 line intensities determined from theory and experiment, Phys. Rev. Lett. 114 (2015) 243001, http://dx.doi.org/10.1103/PhysRevLett.114.243001.

[51] E.J. Zak, J. Tennyson, O.L. Polyansky, L. Lodi, N.F. Zobov, S.A. Tashkun, V.I. Perevalov, Room temperature line lists for CO_2 symmetric isotopologues with *ab initio* computed intensities, J. Quant. Spectrosc. Radiat. Transfer 189 (2017) 267–280, http://dx.doi.org/10.1016/j.jqsrt.2016.11.022.